Water Vapour Climate Change Initiative (WV_cci) - CCI+ Phase 2

ATBD Part 3 - Merged CDR-3 and CDR-4 products

Ref: D2.2

Date: 27 June 2023

Issue: 3.0

For: ESA / ECSAT

Ref: CCIWV.REP.022

This Page is Intentionally Blank

Project	**:**	**Water Vapour Climate Change Initiative (WV_cci) - CCI+ Phase 2**
Document Title:		**ATBD Part 3 - Merged CDR-3 and CDR-4 products**
Reference	**:**	**D2.2**
Issued	**:**	**27 June 2023**
Issue :		**3.0**
Client:		**ESA / ECSAT**

Author(s)	**:**	Michaela Hegglin and Hao Ye (UoR)

Copyright	**:**	Water_Vapour_cci Consortium and ESA

Document Change Log

Issue/ Revision	Date	Comment
1.0	13 August 2020	Issue 1 at end of year 2 phase 1
1.1	13 October 2020	Updated according to RIDs on v1.0
2.0	7 June 2022	Issue 2 at end of year 3 phase 1
3.0	27 June 2023	Issue 3 at end of year 1 of phase 2

TABLE OF CONTENTS

INDEX OF FIGURES

1. INTRODUCTION

1.1 Purpose

This document presents the algorithm theoretical baseline document (ATBD) for the merged VRWV CDR-3 v4.0 and CDR-4 v2.0 products as produced within Phase 2 of the ESA Water_Vapour_cci project. The purpose of the ATBD is to provide detailed information on the physical, mathematical and functional descriptions used in the merging algorithms for the two products and also their input datasets.

1.2 Structure of the document

This ATBD is structured as follows:

- Algorithm definition for CDR-3 and SPARC Data Initiative climatology input fields (Section 2)

- Algorithm definition for CDR-4 (Section 3)

- Summary and Conclusions (Section 4).

2. ALGORITHM DEFINITION CDR-3

2.1 Introduction

The ESA WV_cci CDR-3 features a long-term zonal monthly mean dataset of vertically resolved water vapour (VRWV) that consists of a merger between the satellite limb sounders SAGE II, UARS-MLS, HALOE, POAM III, SMR, SAGE III, SCIAMACHY, MIPAS, ACE-FTS, ACE-MAESTRO, Aura-MLS and SAGE III/ISS. A main goal of the construction of this CDR was the focus on correcting for spatio-temporal sampling differences and biases between input datasets.

2.2 Heritage

The methodological approach that has been used as basis for the WV_cci CDR-3 merging algorithm had been developed by Hegglin et al. (2014) [RD-1]. This merging method uses the stratospheric water vapour fields of a chemistry–climate model nudged to observed meteorology as a transfer function between different satellite instruments. This approach has been shown to overcome issues arising from short overlap periods and instrument drifts, which are more likely towards the end of mission lifetimes when satellite instruments can suffer degradation and satellite orbits start to drift.

2.3 SPARC Data Initiative climatology construction

As input data to CDR-3, the SPARC Data Initiative monthly zonal mean climatologies are being used. More instrument-specific information on these input datasets can be found in SPARC (2017) [RD-2], Hegglin et al. (2013) [RD-3], and Hegglin et al. (2021) [RD-4], but we here give a short general summary of how the climatologies are constructed.

Monthly zonal mean time series of water vapour have been calculated for fields on the SPARC Data Initiative climatology grid, using 5° latitude bins (with mid-points at -87.5°, -82.5°, -77.5°, …, 87.5°) and 28 pressure levels (300, 250, 200, 170, 150, 130, 115, 100, 90, 80, 70, 50, 30, 20, 15, 10, 7, 5, 3, 2, 1.5, 1, 0.7, 0.5, 0.3, 0.2, 0.15 and 0.1 hPa). Water vapour is reported as volume mixing ratios (VMR) along with the 1-σ standard deviation, the number of averaged data values given for each month, latitude bin, and pressure level. In addition, the mean, minimum, and maximum local solar time (LST), average day of the month, and average latitude of the data within each bin for one selected pressure level are also provided (see Figure 2-1).

Original data have been carefully screened according to recommendations given in relevant quality documents, in the published literature, or according to the best knowledge of the involved instrument scientists. Monthly zonal mean products are calculated as the average of all of the measurements on a given pressure level within each latitude bin and month. An exception is MIPAS, for which measurements are interpolated to the centre of the latitude bin after averaging. For some instruments, averaging was done in log10(VMR) space. If not otherwise mentioned, a minimum of five measurements within the bin is required to calculate a monthly zonal mean for each instrument.
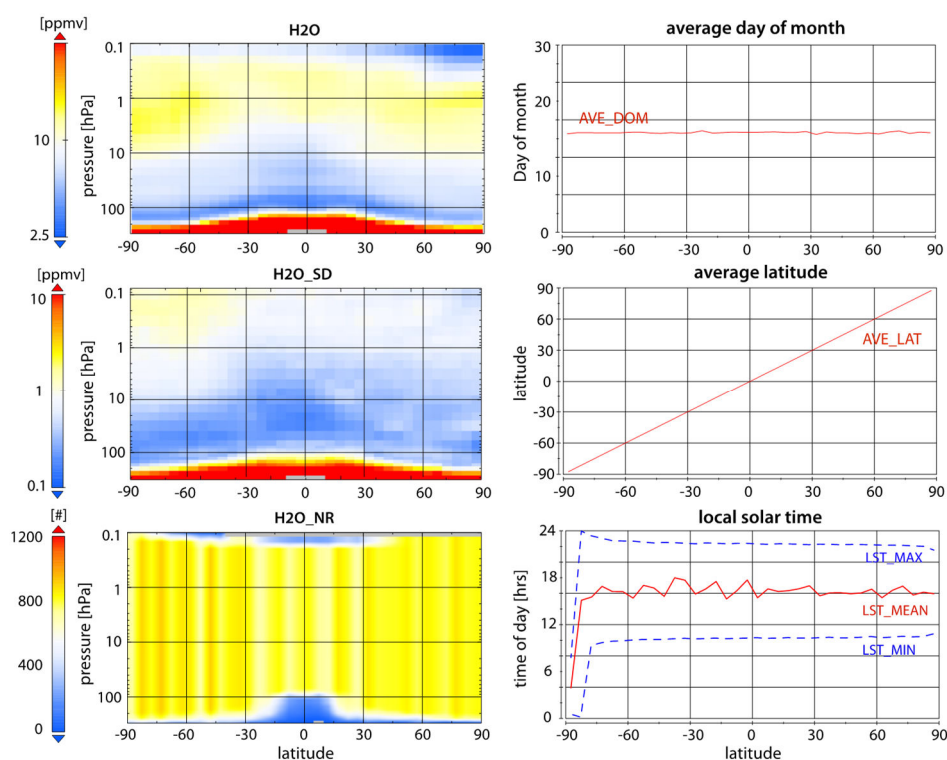
Figure 2-1: Example of SPARC Data Initiative climatology variables. The example shown here is for MIPAS April 2008.

2.4   CDR-3 merging algorithm

The merging algorithm is described in detail in Hegglin et al. (2014) [RD-1] and summarised here. It consists of the following steps that are also exemplified in Figure 2-2:

- The monthly zonal mean SPARC Data Initiative data of the individual instruments described in Section 2.3, are used as input to the merging algorithm.

- For each instrument (i), latitude grid, and pressure level, a mean offset between the observed and modelled water vapour time series is calculated as an average over the full mission (i.e. without time-dependency) according to

$$d[H_2O]_i = \langle [H_2O]_i \rangle - \langle [H_2O]_{CCM} \rangle \qquad \text{(Equation 1)}$$

  where i denotes a given instrument and *CCM* a chemistry–climate model nudged to observed meteorology.

- In a second step, each time series is bias-corrected with respect to a reference (here calculated as the average of Aura-MLS, MIPAS, and ACE-FTS) using the biases calculated according to Equation 1 for both instrument i and reference *Ref.* The resulting bias-corrected water vapour concentration for each instrument ($[H_2O]_{i\_bc}$) can thereby be expressed as:

$$[H_2O]_{i\_bc} = [H_2O]_i - d[H_2O]_i + d[H_2O]_{Ref} \qquad \text{(Equation 2)}$$

- In a third step, the bias-corrected water vapour time series are being scanned for unphysical values (that is negative values), detected outliers are filtered out, and the remaining data points are merged to a bias-corrected monthly mean using an optimal estimation approach to merge the multi-instrument data points (`merged`):

$$[H_2O]_{merged} = \sum_{i=1}^{N} \alpha_i [H_2O]_{i_{bc}} \left(\sum_{i=1}^{N} \alpha_i \right)^{-1} \qquad \text{(Equation 3)}$$

  where *N* denotes the number of instruments available, and α_i is the weighting factor for each instrument. Currently, α_i is calculated as the moment of each instrument's bias-corrected differences (seen in Figure 2-2, panel c).

As shown in Figure 2-2, the biases between the individual instrument time series have been removed after step 2.

Each step in the procedure has gone through visual inspection so to ensure correct functioning of the merging algorithm, which has been continuously automated. The implementation of an optimal estimation approach for the merging is the most innovative improvement of the merging methodology put forward by Hegglin et al. (2014) [RD-1] and provides a first essential step towards dealing with inconsistent seasonal cycle amplitudes, outliers, and sampling issues that may affect anomalies. However, these points are being further investigated during WV_cci Phase 2.
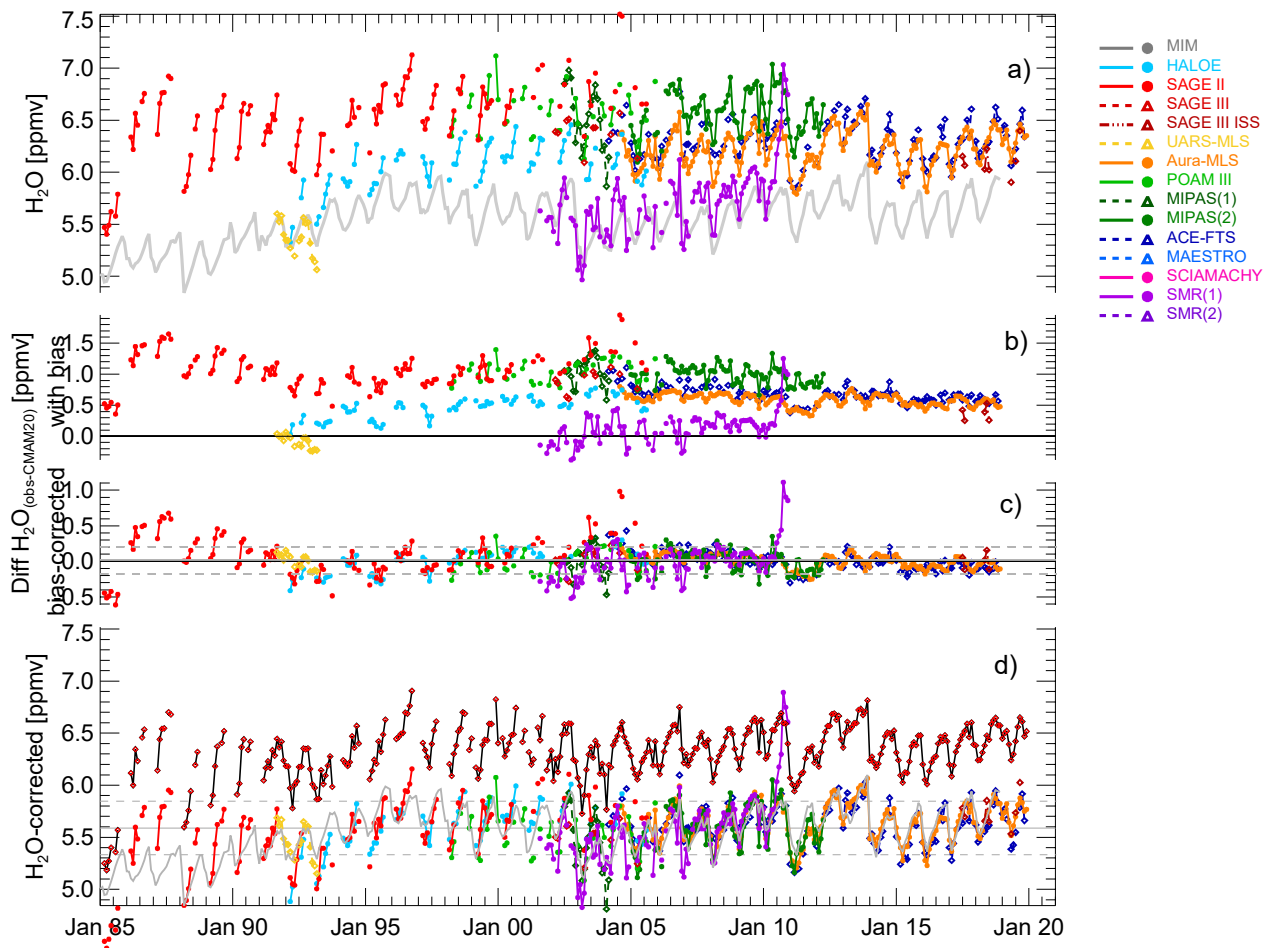
Figure 2-2: Steps involved in the merging algorithm of CDR-3. (a) The water vapour time series of the different instruments are given in colours (see legend), the CCM in grey. (b) Instrumental differences to the CCM, here CMAM is used. (c) Bias-corrected instrument offsets. (d) Bias-corrected instrument time series and final merged dataset (black line with red diamonds) transferred back to the instrumental reference (average of Aura-MLS, ACE-FTS, and MIPAS).

2.5   Assumptions and limitations

The main assumption underlying the merging methodology is that the quality of the chemistry–climate model simulation is sufficient so as not to introduce spurious trends into the merged observational time series. This seems justified, since all the transfer function does is to shift a given instrument record by an absolute amount and does not affect the time series evolution in any other way. We have so far used the Canadian Middle Atmosphere Model CMAM as transfer function, since its stratospheric transport has been tested rigorously and its representation of other trace gases has been shown to be promising (e.g., Shepherd et al., 2014 [RD-5]). This assumption will, however, need to be further tested in WV_cci Phase 2 by using different models as transfer function that are known to show somewhat different behaviour (e.g. Lossow et al., 2018 [RD-6]).

The implementation of the optimal estimation approach in the final merging step was newly introduced in phase 1 of the project and underwent further testing during phase 2. Overall, the OE method produces reasonable results as found in evaluations, which will be presented in an updated PVIR during year 2. However, the choice of using the mean bias-corrected differences as weighting in the optimal estimation equation, is found to be biasing the merged WV record towards the model concentrations and thus should be replaced with a different approach (to be decided). The solution to this problem will be investigated further in WV_cci Phase 2.

3.   ALGORITHM DEFINITION CDR-4

3.1   Introduction

The objective of ESA WV_cci CDR-4 is to construct a prototype three-dimensional vertically resolved water vapour dataset in the upper troposphere and lower stratosphere (UTLS) region by merging both limb- and nadir-viewing satellite observations from Aura-MLS, MIPAS and IMS. The nadir-viewing geometry delivers reliable VRWV profiles with high precision mainly in the troposphere and the limb-viewing geometry mainly covers VRWV profiles in the stratosphere and above. In the UTLS region, due to the very strong vertical gradients in water vapour concentrations, both types of viewing geometries lead to large uncertainties. The merged prototype product CDR-4 takes advantages from these two types of viewing geometry to improve the quality of the VRWV profile data in this region.

The methodology used for the merging of observations from the two viewing geometries developed in Phase 1 is applying a bias-correction relative to *in situ* VRWV profiles from balloon-borne hygrometer (BBH, same as FPH/CFH) observations. All the input data are bias-corrected via a quantile-mapping technique (Maraun, 2013 [RD-7]) and turned into a harmonised limb/nadir data record of VRWV in the UTLS region. These harmonised VRWV data from multiple satellite instruments are then merged into a three-dimensional VRWV product CDR-4.

In project Phase 1, the prototype merged CDR-4 data was produced for the period of 2010-2014. As planned, the merged CDR-4 will be further extended backwards and forwards to cover the period of 2007-2023 with the merging algorithm described above. This merging algorithm was, however, to be improved by adopting new reference profiles to compensate for the limited representativity of the BBH profiles. However, the proposed ACE-FTS and ACE-MAESTRO profiles were found to be too dry in the UTLS as a reference to bias-correct other satellite observations, hence the ACE profiles are deemed not suitable in the bias-correction procedure, similarly to the balloon-borne hygrometer profiles. Other new potential reference profiles will be investigated further in Phase 2.

As proposed in Phase 2, alternative merging techniques will be additionally investigated for the merging of the CDR-4 product. As an alternative merging technique, the approach employed for data merging in CDR-3 (using a CCM as transfer function) is investigated based on CMAM simulations. Currently, the WV simulations from CMAM are compared to global WV

data from ERA5 and local WV data from BBH profiles. This work is ongoing and will be updated in the next update of this document.

3.2 Bias-correction on water vapour profiles

The original retrieved water vapour profiles consist of limb measurements from Aura-MLS and MIPAS instruments and the nadir data product IMS (which is based on a combination of IASI, MHS and AMSU satellite measurements). As mentioned in Section 3.1, the input VRWV profiles from different satellite instruments will be bias-corrected via a quantile-mapping technique in comparison to reference data from BBH observations. Limited to the spatial and temporal coverage of the BBH observations, the comparisons are performed in a common geophysical reference coordinate system – here, the thermal tropopause height is chosen – to reduce geophysical noise.

Figure 3-1 shows the comparison of VRWV profiles from different satellites to reference datasets in a geophysical-based vertical coordinate system (here, using the thermal tropopause as reference). Due to limited spatial and temporal coverage, JULIA aircraft data is not used in the bias-correction process and only BBH profile observations are chosen as reference data (see DARD [RD-8]). The comparisons to BBH profile data clearly show that the limb WV data match well with hygrometer profiles above the tropopause and the nadir VRWV data from IMS agree better with the hygrometer profiles below the tropopause. Due to the limitation of the spatial and temporal coverage, the highly sparse ACE-FTS and ACE-MAESTRO are not included in the production of CDR-4 data.

In Figure 3-1, all profiles from satellites and BBH are screened with quality control suggestions from each instrument. It is noteworthy to mention that the comparison is carried out in five latitude bands: 90°S–60°S, 60°S–30°S, 30°S–30°N, 30°N–60°N, and 60°N–90°N, due to the limitation of the sparse BBH observations. The following bias-correction process will also be performed in each latitude band. As there is no BBH site in the latitude band 90°S–60°S, the original profiles from all satellite observations are used in the production of CDR-4 data in this band. The choice of these latitude bands leads to the problem with tropospheric/stratospheric intrusions around 30° in latitude, in the case of double thermal tropopause. In practice, only the lowest thermal tropopause is used in this study and the tropopause height of 14 km is chosen as the limit to deal with tropospheric/stratospheric intrusions. The tropical profiles (30°S–30°N) with a tropopause height less than 14 km are treated as stratospheric intrusions from mid-latitude and assigned into mid-latitude bands. Conversely, the mid-latitude profiles with a tropopause height larger than 14 km are regarded as tropospheric intrusions from tropical regions and assigned into the tropical band. This latitude correction on the profiles

leads to a remarkable reduction of variation within the mean water vapour profiles in the tropopause-based coordinate.
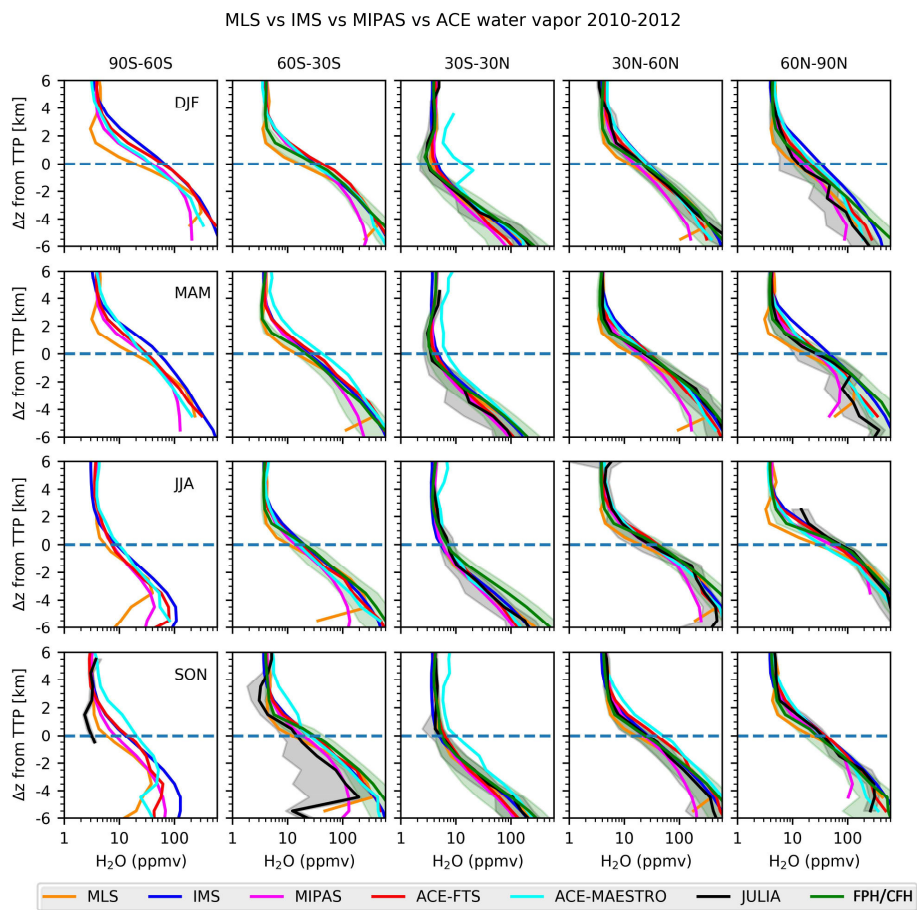
Figure 3-1: Comparison of water vapour vertical profiles relative to thermal tropopause height from different satellite instruments and in-situ observations. The satellite observations are from the period 2010 to 2012, and the JULIA and FPH/CFH data from the period 2000 to 2016. From top to bottom: DJF, MAM, JJA and SON. From left to right: 90°S–60°S, 60°S–30°S, 30°S–30°N, 30°N–60°N, and 60°N–90°N. The water vapour mixing ratio is calculated for each 1 km altitude bin from -6 to +6 km range, with the mid-points of the altitude grid boxes at -5.5, -4.5, -3.5,…, +5.5 km, respectively. The grey and green shadings show the mean absolute deviation (MAD) of the mean mixing ratio from JULIA (black) and FPH/CFH (green), respectively.

3.2.1 Bias-correction with BBH observations

The bias-correction algorithm is applied to VRWV profiles from each satellite instrument in the tropopause-based vertical coordinate. For each month and latitude band (see Figure 3-1), the

VRWV biases between each satellite instrument and BBH observations are calculated using a quantile-mapping technique for each 1 km altitude bin within the -6 to +6 km range. For each altitude bin in each month, the biases are computed through the cumulative distribution function (CDF) for the WV measurements as:

$$WV_{k,corrected} = F_{BBH}^{-1}[F_k(WV_k)], \qquad \text{(Equation 4)}$$

where the F_{BBH}^{-1} is the inverse CDF for BBH observations and F_k is the CDF for the input data from each satellite instrument. Note that the WV_k here is taken as the logarithm of the mixing ratio. As the quantile-mapping technique uses the quantile–quantile matching to converge the satellite WV distribution function to the BBH one, the biases between WV profiles from each satellite instrument and BBH observations are calculated for each quantile. These biases are applied back to the original satellite VRWV profiles on the original vertical levels. Figure 3-2 shows an example of the distribution of bias-corrected WV measurements from MLS in the range 2–3 km below the tropopause in the tropical region. It indicates that the bias-corrected WV from each satellite instrument has a much better agreement with the BBH observations. As mentioned above, in the latitude range 90S–60S, the bias-correction is not available due to lack of BBH observations. Note, this will introduce a discontinuity in the dataset and an associated increase in measurement uncertainty.
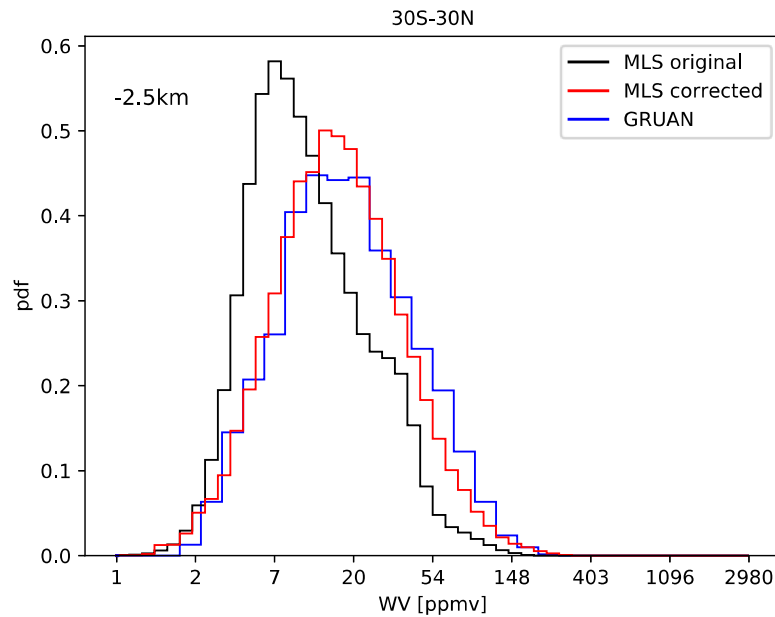
Figure 3-2: Example for the bias-correction method with the quantile-mapping technique with the MLS measurements.

For creating monthly mean data for the individual instruments, the bias-corrected VRWV profiles are taken for a temporal and spatial level 3 aggregation. The aggregation is performed

for each month in 2010–2014 with a horizontal resolution of 5 degrees by 5 degrees in latitude and longitude. In the vertical dimension, the L2 VRWV profiles are interpolated to 26 pressure levels from 1000 hPa up to 10 hPa (1000, 950, 900, 850, 800, 750, 700, 650, 600, 550, 500, 450, 400, 350, 300, 250, 225, 200, 175, 150, 125, 100, 70, 50, 30, 10 hPa), as also specified in the PSD [RD-9]. For all sensors, the monthly average is computed as the mean of VRWV profiles $q_k(x, y, z)$:

$$q(x, y, z) = \frac{1}{N} \sum q_k(x, y, z),$$ (Equation 5)

where N is the number of measurements. Note that for IMS, the average VRWV is calculated based on the logarithm of mixing ratio, same as the original VRWV profiles. The uncertainty of the monthly mean σ_q can be estimated as the standard error of the mean:

$$\sigma_q(x, y, z) = \sqrt{S^2(x, y, z)/N},$$ (Equation 6)

where $S^2(x, y, z)$ is the variance of the WV measurements calculated as:

$$S^2(x, y, z) = \frac{1}{N-1} \sum [q_k(x, y, z) - q(x, y, z)]^2.$$ (Equation 7)

Figure 3-3 shows an example of bias-correction of the MLS observations and comparison against reanalyses (ERA5 and MERRA2) for the period of 2010 to 2014. The bias-correction method can increase the water vapour in the upper troposphere, which is known to be too dry in the original observations.
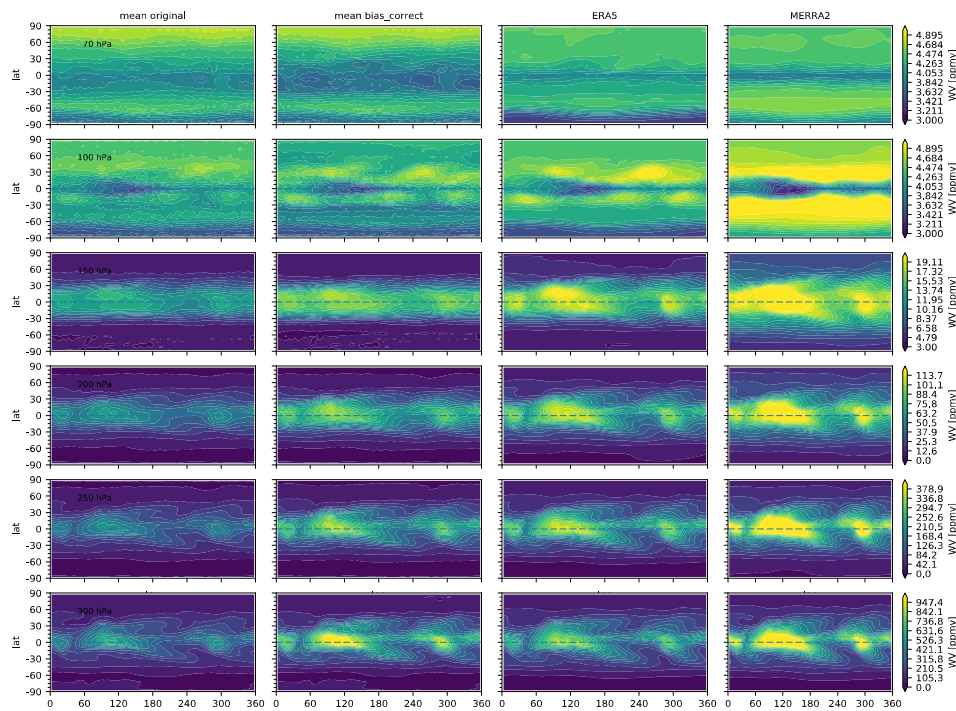
Figure 3-3: Example of bias-correction on MLS observation with reference to BBH profiles. Figure shows the water vapour horizontal distribution at pressure levels from top to bottom: 70 hPa, 100 hPa, 150 hPa, 200 hPa, 250 hPa, and 300 hPa. From left to right, the data are from: original satellite mean, bias-corrected satellite mean, ERA-5, and MERRA-2. The water vapour values are averaged from 2010 to 2014.

3.2.2 Bias-correction with ACE-FTS observations

In Phase 2, the WV observations from ACE-FTS were proposed to be used as new reference data in the bias-correction procedure. Same as the processing in Section 3.2.1 with BBH as the reference, satellite observations in the period of 2010-2014 are bias-corrected with ACE-FTS profiles obtained during 2004-2019. Figure 3-4 shows the example of bias-correction on MLS WV data with ACE-FTS profiles and further comparison with reanalyses. The bias-correction with ACE-FTS tends to reduce the WV in the upper troposphere, especially over the tropical region during summer, which is opposite to the bias-correction based on BBH profiles. This confirms a low-bias found in ACE-FTS observations in the upper troposphere (RD-13) and that the ACE-FTS profiles are not suitable to improve the merging algorithm with reference to BBH profiles (at least in the upper troposphere). Thus, other new reference profiles should be explored or alternative merging techniques should be investigated.
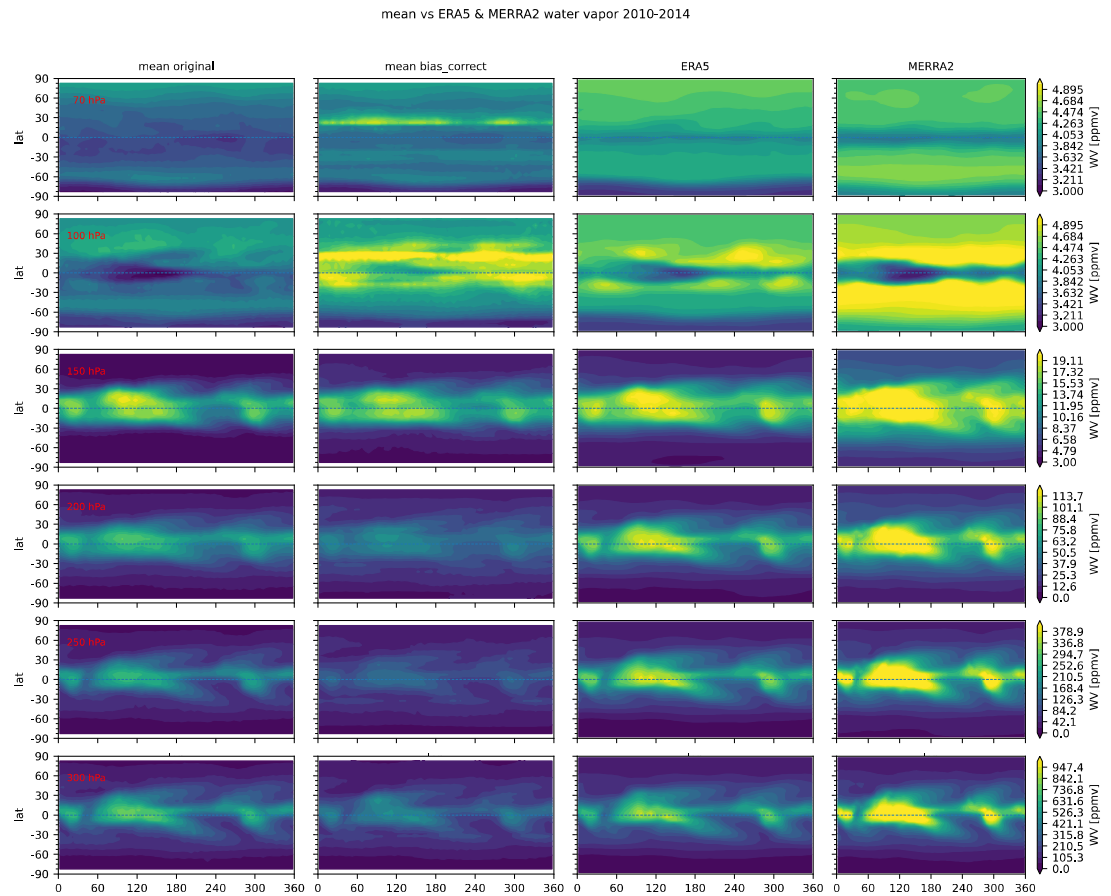
Figure 3-4: Same as Figure 3-3 but for bias-correction on MLS observation with reference to ACE-FTS profiles.

3.3   CDR-4 merging algorithm

The merged monthly mean dataset of VRWV profiles is created from several satellite instruments: limb VRWV data from Aura-MLS and MIPAS and nadir VRWV data from RAL IMS. The monthly mean data from individual instruments, which are described in Section 3.2, are here used to calculate the merged monthly mean VRWV CDR-4. Due to the limited spatial coverage of BBH observations, the merged product consists of a combination of original VRWV and bias-corrected VRWV profiles at different pressure levels following the merging rules given below:

- at and above 100 hPa (lower stratosphere), only original VRWV monthly mean data from MLS and MIPAS before bias-correction are used to calculate the average;

- between 100 hPa and 300 hPa, the bias-corrected VRWV monthly mean data of all instruments are used to calculate the average;

- below 300 hPa (troposphere), only original VRWV monthly mean data from IMS before bias-correction are used to calculate the average.

In the lower stratosphere, the amount of BBH observations is not enough for a reliable bias-correction to the limb satellite observations and the original limb WV has a relatively high accuracy, thus the bias-corrected data are not included in the merged product. In the troposphere, the original nadir VRWV profiles retrieved from IMS also show very high accuracy and only the original month mean data are used in the merged product. An example of the merged VRWV CDR-4 product is shown in Figure 3-5.
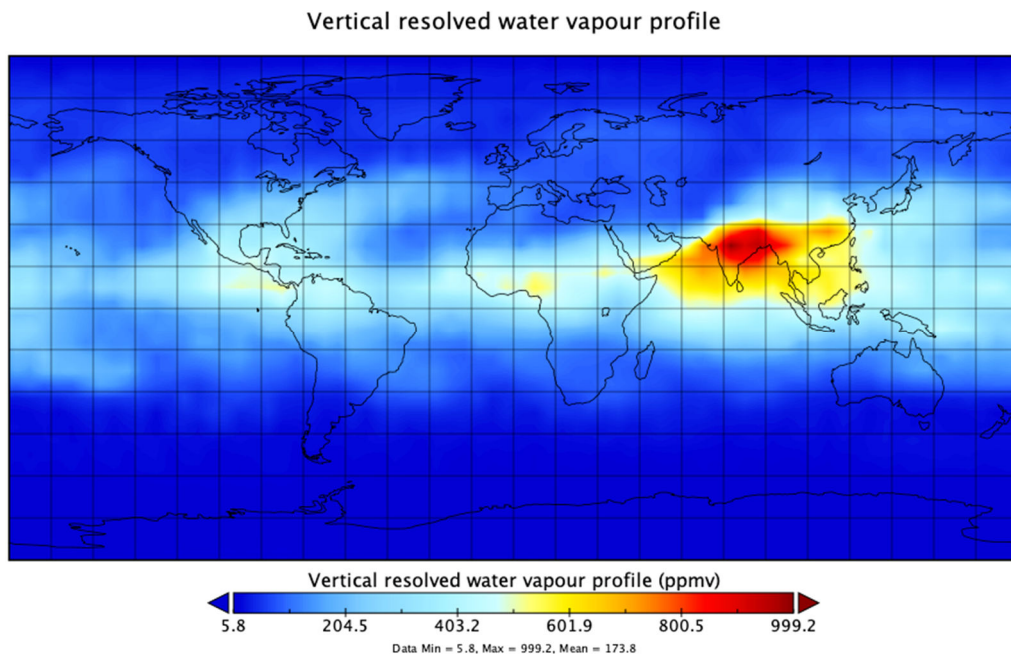
Figure 3-5: Merged VRWV monthly product at 250 hPa for July 2010.

All data are included in one NetCDF4 file, which includes the merged data and the corresponding uncertainty for each grid point.

3.4 Assumptions and limitations

The main assumption in the algorithm to construct the VRWV CDR-4 product in the UTLS region is that VRWV profiles from BBH observations are representative for the bias-correction applied to the VRWV data from satellite instruments. Due to the limited spatial and temporal coverage of the BBH observations, a bias-correction of the VRWV profile data based on a validation with coincident BBH observations is not feasible. Instead, the tropopause height, a

meteorological feature that determines the structure found in UTLS water vapour [RD-10–RD-14], is chosen as the geophysical reference coordinate system in the vertical. In this new tropopause-based coordinate system, the biases in VRWV can be calculated between satellite instruments, and BBH observations including VRWV data obtained over a larger geographical domain. With the bias-correction applied to the VRWV data from satellite instruments, it is possible to merge together the VRWV profiles from both limb- and nadir-viewing geometries into a single data product. It is highlighted here that the merging approach is assumed to mostly correct for the smoothing characteristics of the averaging kernels of the respective instruments.

For this prototype CDR-4 product, there are still several limitations:

1. Biases between satellite data and BBH observations in the geophysical reference coordinate system are calculated within several broad latitude bands, thus the longitudinal variations of these biases may not be fully accounted for in this process. It should also be noted that in latitude bands where no BBH observations are available, the lack of a bias-correction may currently lead to discontinuities between adjacent latitude bands. Tests on the bias-correction algorithm with ERAi reanalysis WV data show that the spatial and temporal coverage of the reference data have a notable impact on the quality of bias-correction to the satellite profiles. Thus, more frequent and denser BBH observations (or an alternative instrument reference) are needed across the globe for a quantitatively better bias-correction for the satellite observations. New tests introducing ACE-FTS profiles as add-on reference data in the bias-correction procedure suggest that the ACE-FTS profiles tends to be too dry over the tropical region in the upper troposphere. Different reference profiles or a different combination (e.g., ACE in the extratropical lowermost stratosphere and tropical tropopause region down to 150 hPa and BBH in the tropical upper troposphere), should be explored.

2. The satellite instruments show a big difference in the amount of VRWV profile measurements across the UTLS. The proportional contribution of each satellite observations to the merged CDR-4 product is important to the final data quality. An appropriate weighting scheme to the satellite data based on the derived input quality and derived instrument-dependent biases is essential for improving the final product quality.

3. The merging rules are likely to bring in a discontinuity in the merged CDR-4 product at 300 and 100 hPa. Assessment of this merging problem shows that there is no need for post-processing at 100 hPa due to the high quality of instrument WV values and

variations. Meanwhile, a smoothing process is applied to VRWV profiles across the 300-hPa level for IMS based on a window function, here using the Blackman window. The smooth processing reduces the sharp discontinuity at 300 hPa between original and bias-correction profiles. To obtain a harmonised and continuous WV data in the vertical, the bias-correction for and merging process of satellite VRWV profiles should be performed throughout the UTLS and troposphere in the future.

4. SUMMARY AND CONCLUSIONS

For CDR-3, the merging algorithm by Hegglin et al. (2014) [RD-1] has been further developed towards operational implementation. In particular, the optimal estimation theory as new approach for the merging of the different satellite instrument inputs has been further evaluated and found robust (apart from the use of the weighting factors based on the mean-differences from the model). While this merging approach addresses many instrumental issues identified as potential problems in the merging process, others still need further implementation and will be the focus of continued improvements of CDR-3 in WV_cci Phase 2. However, the final quality of the dataset is limited mainly by the temporal and spatial coverage of the limb satellite input data, especially in the early years of the instrumental record as is detailed in the PVIR [RD-15]. Here, the quality of other historical limb satellite datasets is being explored to see whether they can be used to fill gaps and extend CDR-3 into the past back to 1978.

For CDR-4, a new prototype merging algorithm is under development that applies a novel bias-correction methodology (quantile mapping) to the input profiles before merging. This methodology accounts for biases in the limb and nadir satellite sounders across the UTLS region, including the smoothing resulting from averaging kernels that are too broad to resolve the vertical gradients found in WV across this region. While the merging algorithm has been found to be promising, limitations arise from a too-scarce spatio-temporal coverage in the reference datasets used for the bias-correction (BBH observation stations). Alternative merging technique, such as the approach employed for data merging in CDR-3 (using a CCM as transfer function) is undergoing. Currently, the WV simulations from CMAM are investigated for the potential transfer function in the bias-correction procedure on the satellite observation for the production of CDR-4.

APPENDIX 1: REFERENCES

RD-1. Hegglin, M. I., D. Plummer, J. Scinocca, T. G. Shepherd, J. Anderson, L. Froidevaux, B. Funke, D. Hurst, A. Rozanov, J. Urban, T. v. Clarmann, K. A. Walker, R. Wang, S. Tegtmeier, and K. Weigel, Variation of stratospheric water vapour trends with altitude from merged satellite data, *Nature Geoscience*, doi: 10.1038/NGEO2236, 2014.

RD-2. SPARC, 2017: The SPARC Data Initiative: Assessment of stratospheric trace gas and aerosol climatologies from satellite limb sounders. By M. I. Hegglin and S. Tegtmeier (eds.), *SPARC Report No. 8*, WCRP-5/2017, doi:10.3929/ethz-a-010863911.

RD-3. Hegglin, M.I., Tegtmeier, S., Anderson, J., Froidevaux, L., Fuller, R., Funke, B., Jones, A., Lingenfelser, G., Lumpe, J., Pendlebury, D. and Remsberg, E., SPARC Data Initiative: Comparison of water vapor climatologies from international satellite limb sounders. *J. Geophys. Res.: Atmospheres*, *118*(20), pp.11-82, 2013.

RD-4. Hegglin, M. I., Tegtmeier, S., Anderson, J., Bourassa, A. E., Brohede, S., Degenstein, D., Froidevaux, L., Funke, B., Gille, J., Kasai, Y., Kyrölä, E. T., Lumpe, J., Murtagh, D., Neu, J. L., Pérot, K., Remsberg, E. E., Rozanov, A., Toohey, M., Urban, J., von Clarmann, T., Walker, K. A., Wang, H.-J., Arosio, C., Damadeo, R., Fuller, R. A., Lingenfelser, G., McLinden, C., Pendlebury, D., Roth, C., Ryan, N. J., Sioris, C., Smith, L., and Weigel, K.: Overview and update of the SPARC Data Initiative: comparison of stratospheric composition measurements from satellite limb sounders, Earth Syst. Sci. Data, 13, 1855–1903, https://doi.org/10.5194/essd-13-1855-2021, 2021.

RD-5. Shepherd, T.G., Plummer, D.A., Scinocca, J.F., Hegglin, M.I., Fioletov, V.E., Reader, M.C., Remsberg, E., Von Clarmann, T. and Wang, H.J., Reconciliation of halogen-induced ozone loss with the total-column ozone record. *Nature Geoscience*, *7*(6), pp.443-449, 2014.

RD-6. Lossow, S., Hurst, D. F., Rosenlof, K. H., Stiller, G. P., von Clarmann, T., Brinkop, S., Dameris, M., Jöckel, P., Kinnison, D. E., Plieninger, J., Plummer, D. A., Ploeger, F., Read, W. G., Remsberg, E. E., Russell, J. M., and Tao, M.: Trend differences in lower stratospheric water vapour between Boulder and the zonal mean and their role in understanding fundamental observational discrepancies, Atmos. Chem. Phys., 18, 8331–8351, https://doi.org/10.5194/acp-18-8331-2018, 2018.

RD-7. Maraun, D., 2013: Bias Correction, Quantile Mapping, and Downscaling: Revisiting the Inflation Issue. J. Climate, 26, 2137–2143, https://doi.org/10.1175/JCLI-D-12-00821.1.

RD-8. ESA CCI Water Vapour: Data Access Requirement Document. M. Schröder, M. Hegglin, H. Brogniez, J. Fischer, D. Hubert, A. Laeng, R. Siddans, C. Sioris, G. Stiller, T. Trent, K. Walker, O. Danne, U. Falk and H. Ye. Issue 3.2, 27 July 2021.

RD-9. ESA CCI Water Vapour: Product Specification Document. M. Schröder, M. Hegglin, O. Danne, J. Fischer, A. Laeng, R. Siddans, C. Sioris, G. Stiller and K. Walker. Issue 3.2, 27 July 2021.

RD-10. Hoor, P., C. Gurk, D. Brunner, M. I. Hegglin, H. Wernli, and H. Fischer (2004): Seasonality and extent of extratropical TST derived from in-situ CO measurements during SPURT, Atmos. Chem. Phys., 4, 1427–1442.

RD-11. Hegglin, M. I., D. Brunner, Th. Peter, P. Hoor, H. Fischer, J. Staehelin, M. Krebsbach, C. Schiller, U. Parchatka, and U. Weers (2006): Measurements of NO, NOy, N2O, and O3 during SPURT: Implications for transport and chemistry in the lowermost stratosphere, Atmos. Chem. Phys., 6, 1331-1350.

RD-12. Hegglin, M. I., C. D. Boone, G. L. Manney, T. G. Shepherd, K. A. Walker, P. F. Bernath, W. H. Daffer, P. Hoor, and C. Schiller (2008): Validation of ACE-FTS satellite data in the upper troposphere/lower stratosphere (UTLS) using non-coincident measurements, Atmos. Chem. Phys., 8, 1483–1499.

RD-13. Hegglin, M. I., C. D. Boone, G. L. Manney, and K. A. Walker (2009): A global view of the extratropical tropopause transition layer (ExTL) from Atmospheric Chemistry Experiment Fourier Transform Spectrometer O3, H2O, and CO, J. Geophys. Res., 114, D00B11, doi: 10.1029/2008JD009984.

RD-14. Schwartz, M. J., G. L. Manney, M. I. Hegglin, N. J. Livesey, M. L. Santee, W. H. Daffer, Climatology and variability of trace gases in extratropical double-tropopause regions from MLS, HIRDLS, and ACE-FTS measurements, J. Geophys. Res. Atmos., 120, doi:10.1002/2014JD021964, 2015.

RD-15. ESA CCI Water Vapour: Product Validation and Intercomparison Report, Part 2. H. Ye, M. Hegglin, M.Schröder, A. Niedorf. Issue 2.0, 1 June 2022.

APPENDIX 2: GLOSSARY

Term	Definition
ACE-FTS	Atmospheric Chemistry Experiment Fourier Transform Spectrometer
ACE-MAESTRO	Atmospheric Chemistry Experiment Measurement of Aerosol Extinction in the Stratosphere and Troposphere Retrieved by Occultation
AMSU	Advanced Microwave Sounding Unit
ATBD	Algorithm Theoretical Basis Document
AURA-MLS	Aura Microwave Limb Sounder
BBH	Balloon-borne Hygrometer
CCI	ESA Climate Change Initiative
CCM	Chemistry–Climate Model
CDF	Cumulative Distribution Function
CDR	Climate Data Record
DARD	Data Access Requirement Document
E3UB	End to End ECV Uncertainty Budget
ERA5	ECMWF Reanalysis v5
ERAi	ECMWF Reanalysis - Interim
ESA	European Space Agency
FPH/CFH	Frost-Point Hygrometer / Cryogenic Frost-Point Hygrometers
HALOE	HALogen Occultation Experiment
IASI	Infrared Atmospheric Sounding Interferometer
IMS	Infra-red Microwave Sounder scheme
JULIA	JÜLich In-situ Airborne Data Base
MERRA-2	Modern-Era Retrospective analysis for Research and Applications, version 2
MHS	Microwave Humidity Sounder
MIPAS	Michelson Interferometer for Passive Atmospheric Sounding
POAM	Polar Ozone and Aerosol Measurement
PVIR	Product Validation and Intercomparison Report
SAGE	Stratospheric Aerosol and Gas Experiment
SAGE III/ISS	Stratospheric Aerosol and Gas Experiment III on the International Space Station

Term	Definition
SCIAMACHY	SCanning Imaging Absorption spectroMeter for Atmospheric CartograpHY
SMR	Submillimeter wave Radiometer
SPARC	Stratosphere-troposphere Processes And their Role in Climate
UARS-MLS	Upper Atmosphere Research Satellite Microwave Limb Sounder
UTLS	Upper troposphere and lower stratosphere
VRWV	Vertical Resolved Water Vapour

End of Document